A Multi-Resolution Approach for Enhancing the BCS-Based Imaging of Sparse Scatterers

N. Anselmi, L. Poli, G. Oliveri, and A. Massa

Abstract

In this work, a novel inverse scattering technique is proposed to deal with the imaging of sparse scatterers under the Born approximation. A Bayesian compressive sensing (*BCS*) solver is integrated within an iterative multi-scaling approach (*IMSA*) to exploit the progressively acquired information on the imaged scenario and adaptively improve the reconstruction accuracy and resolution within the identified region of interest (*RoI*).
Selected numerical results are shown in order to assess the potentialities, as well as the limitations, of the proposed imaging methodology.

1 Numerical Assessment

1.1 E-shaped Object, $\ell = 1.5\lambda$

Test Case Description

Direct solver:

- Side of the investigation domain: $L = 6.0\lambda$
- Cubic domain divided in $\sqrt{D} \times \sqrt{D}$ cells
- Number of cells for the direct solver: $D = 1600$ (discretization = $\lambda/10$)

Investigation domain:

- Cubic domain divided in $\sqrt{N} \times \sqrt{N}$ cells
- Number of cells for the inversion:
  - First Step IMSA: $N^{(1)} = 100$ (discretization = $\lambda/10$)
  - Following Steps IMSA: $N^{(i)}$ not fixed, defined according to the estimated RoI $\mathcal{D}^{(i)}$

Measurement domain:

- Total number of measurements: $M = 60$
- Measurement points placed on circles of radius $\rho = 4.5\lambda$

Sources:

- Plane waves
- Number of views: $V = 60$; $\theta_{inc}^{v} = 0^\circ + (v-1) \times (360/V)$
- Amplitude: $A = 1.0$
- Frequency: $F = 300$ MHz ($\lambda = 1$)

Background:

- $\varepsilon_r = 1.0$
- $\sigma = 0$ [S/m]

Scatterer

- E-shaped object, $\ell = 1.5\lambda$
- $\varepsilon_r \in \{1.01, 1.02, 1.04, 1.05, 1.06, 1.08, 1.10, 1.15, 1.20\}$
- $\sigma = 0$ [S/m]

ELEDIA Research Center

1.1.1 E-shaped Object, $\ell = 1.5\lambda$, $\tau = 0.02$ - IMSA-BCS reconstructed profiles

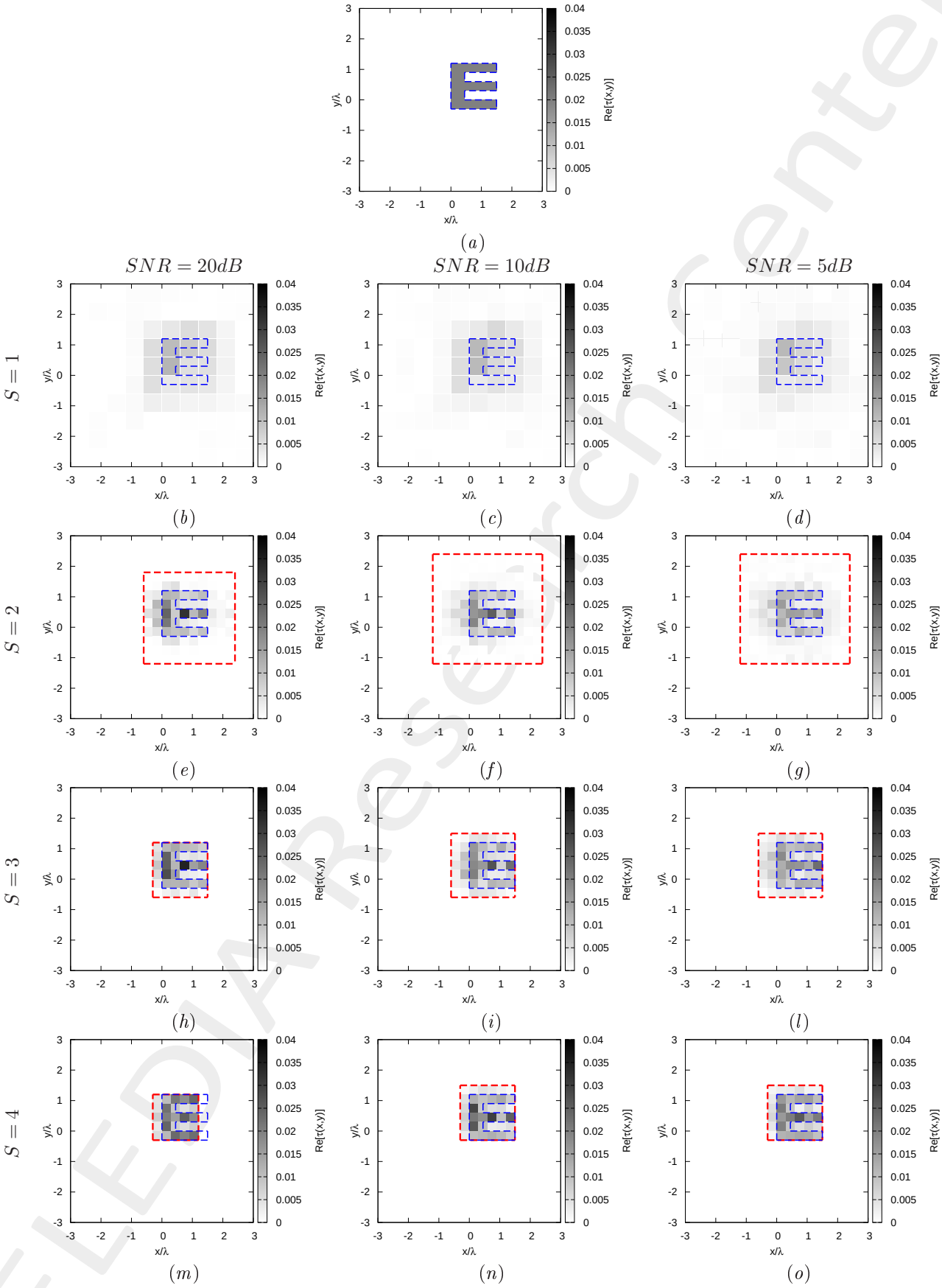

Figure 1: *E-shaped Object*, $\tau = 0.02$ - (a) Actual profile and (b)-(o) IMSA-BCS reconstructed profiles for $(b)(e)(h)(m)$ $SNR = 20$ [dB], $(c)(f)(i)(n)$ $SNR = 10$ [dB] and $(d)(g)(l)(o)$ $SNR = 5$ [dB] at the step (b)-(d) $S = 1$, (e)-(g) $S = 2$, (h)-(l) $S = 3$ and (m)-(o) $S = 4$.

FEDIA Research Center

	$SNR = 50dB$			
	$S = 1$	$S = 2$	$S = 3$	$S = 4$
ξ_{tot}	1.41×10^{-3}	6.09×10^{-4}	5.12×10^{-4}	5.12×10^{-4}
ξ_{int}	1.24×10^{-2}	7.95×10^{-3}	7.76×10^{-3}	7.76×10^{-3}
ξ_{ext}	8.86×10^{-4}	2.62×10^{-4}	1.71×10^{-4}	1.71×10^{-4}
	$SNR = 20dB$			
	$S = 1$	$S = 2$	$S = 3$	$S = 4$
ξ_{tot}	1.41×10^{-3}	6.78×10^{-4}	5.39×10^{-4}	4.53×10^{-4}
ξ_{int}	1.23×10^{-2}	8.64×10^{-3}	7.98×10^{-3}	6.70×10^{-3}
ξ_{ext}	8.95×10^{-4}	3.03×10^{-4}	1.88×10^{-4}	1.56×10^{-4}
	$SNR = 10dB$			
	$S = 1$	$S = 2$	$S = 3$	$S = 4$
ξ_{tot}	1.45×10^{-3}	6.92×10^{-4}	6.35×10^{-4}	5.53×10^{-4}
ξ_{int}	1.24×10^{-2}	8.07×10^{-3}	7.72×10^{-3}	8.04×10^{-3}
ξ_{ext}	9.17×10^{-4}	3.41×10^{-4}	2.99×10^{-4}	1.99×10^{-4}
	$SNR = 5dB$			
	$S = 1$	$S = 2$	$S = 3$	$S = 4$
ξ_{tot}	1.55×10^{-3}	8.26×10^{-4}	6.13×10^{-4}	4.37×10^{-4}
ξ_{int}	1.29×10^{-2}	9.12×10^{-3}	7.05×10^{-3}	5.40×10^{-3}
ξ_{ext}	9.76×10^{-4}	4.22×10^{-4}	3.06×10^{-4}	2.01×10^{-4}

Table I: *E-shaped Object*, $\ell = 1.5\lambda$, $\tau = 0.02$ - Reconstruction errors: total (ξ_{tot}), internal (ξ_{int}) and external (ξ_{ext}) errors.

	$SNR = 50dB$			
	$S = 1$	$S = 2$	$S = 3$	$S = 4$
$L^{(S)}$	6.00	3.00	1.80	1.80
$N^{(S)}$	100	175	175	175
$Q^{(S)}$	100	100	36	36
	$SNR = 20dB$			
	$S = 1$	$S = 2$	$S = 3$	$S = 4$
$L^{(S)}$	6.00	3.00	1.80	1.50
$N^{(S)}$	100	175	175	175
$Q^{(S)}$	100	100	36	25
	$SNR = 10dB$			
	$S = 1$	$S = 2$	$S = 3$	$S = 4$
$L^{(S)}$	6.00	3.60	2.10	1.80
$N^{(S)}$	100	208	208	208
$Q^{(S)}$	100	144	49	36
	$SNR = 5dB$			
	$S = 1$	$S = 2$	$S = 3$	$S = 4$
$L^{(S)}$	6.00	3.60	2.10	1.80
$N^{(S)}$	100	208	208	208
$Q^{(S)}$	100	144	49	36

Table II: *E-shaped Object*, $\tau = 0.02$ - Investigation domain parameters: restricted investigation domain size $L^{(S)}$, total number of cells $N^{(S)}$ and number of cells within the restricted domain size $Q^{(S)}$.

ELEDIA Research Center

1.1.2 E-shaped Object, $\ell = 1.5\lambda$, $\tau = 0.05$ - IMSA-BCS reconstructed profiles

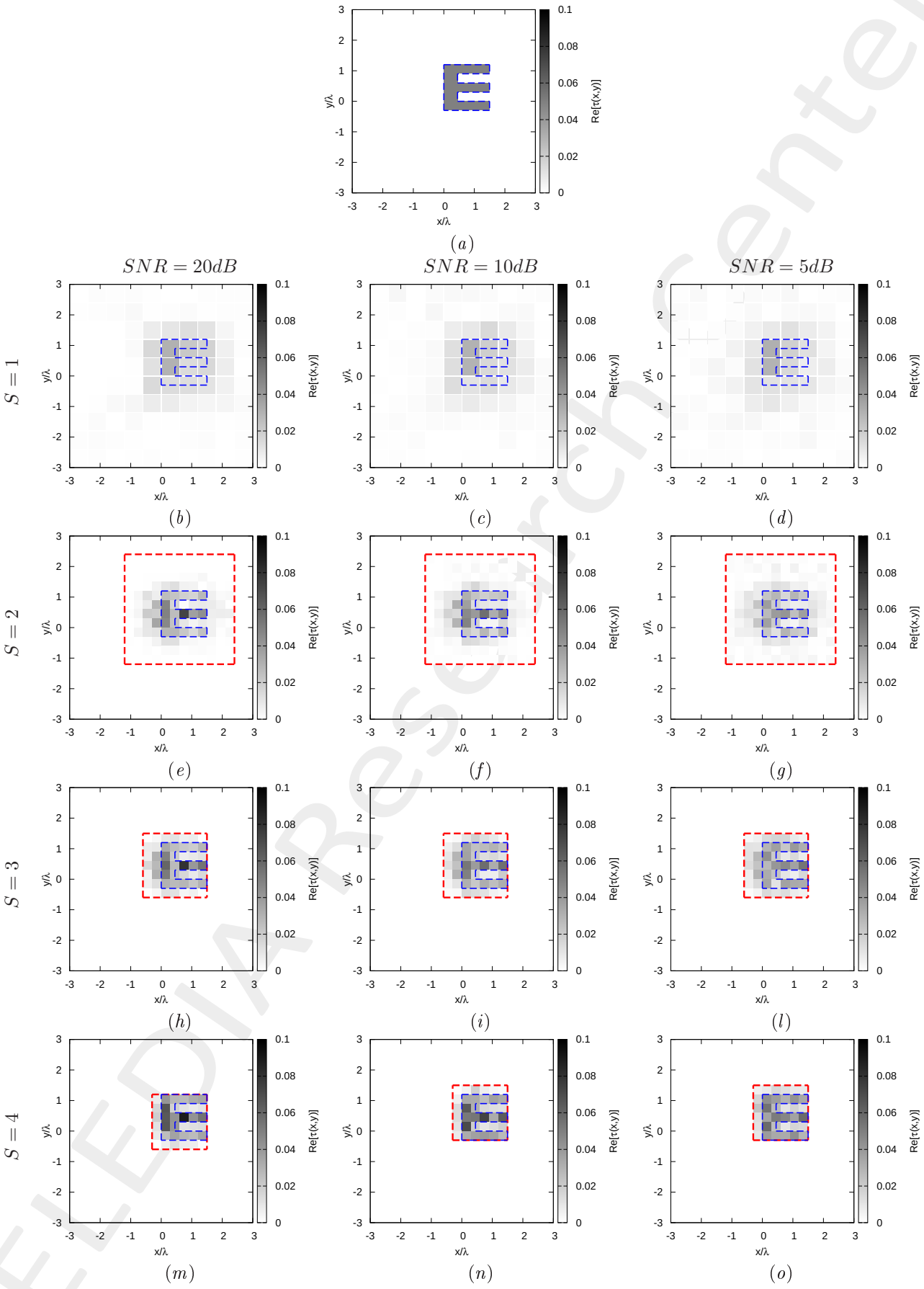

Figure 2: *E-shaped Object*, $\tau = 0.05$ - (a) Actual profile and (b)-(o) IMSA-BCS reconstructed profiles for $(b)(e)(h)(m)$ $SNR = 20$ [dB], $(c)(f)(i)(n)$ $SNR = 10$ [dB] and $(d)(g)(l)(o)$ $SNR = 5$ [dB] at the step (b)-(d) $S = 1$, (e)-(g) $S = 2$, (h)-(l) $S = 3$ and (m)-(o) $S = 4$.

ELEDIA Research Center

	$SNR = 50dB$			
	$S = 1$	$S = 2$	$S = 3$	$S = 4$
ξ_{tot}	3.91×10^{-3}	1.81×10^{-3}	1.18×10^{-3}	1.18×10^{-3}
ξ_{int}	2.74×10^{-2}	1.92×10^{-2}	1.54×10^{-2}	1.54×10^{-2}
ξ_{ext}	2.70×10^{-3}	9.47×10^{-4}	4.92×10^{-4}	4.92×10^{-4}
	$SNR = 20dB$			
	$S = 1$	$S = 2$	$S = 3$	$S = 4$
ξ_{tot}	3.93×10^{-3}	1.92×10^{-3}	1.63×10^{-3}	1.25×10^{-3}
ξ_{int}	2.74×10^{-2}	1.96×10^{-2}	1.80×10^{-2}	1.64×10^{-2}
ξ_{ext}	2.73×10^{-3}	1.04×10^{-3}	8.31×10^{-4}	5.15×10^{-4}
	$SNR = 10dB$			
	$S = 1$	$S = 2$	$S = 3$	$S = 4$
ξ_{tot}	4.04×10^{-3}	2.01×10^{-3}	1.62×10^{-3}	1.20×10^{-3}
ξ_{int}	2.82×10^{-2}	1.90×10^{-2}	1.63×10^{-2}	1.52×10^{-2}
ξ_{ext}	2.78×10^{-3}	1.13×10^{-3}	9.12×10^{-4}	5.25×10^{-4}
	$SNR = 5dB$			
	$S = 1$	$S = 2$	$S = 3$	$S = 4$
ξ_{tot}	4.21×10^{-3}	2.34×10^{-3}	1.67×10^{-3}	1.14×10^{-3}
ξ_{int}	2.87×10^{-2}	2.17×10^{-2}	1.58×10^{-2}	1.10×10^{-2}
ξ_{ext}	2.83×10^{-3}	1.32×10^{-3}	9.64×10^{-4}	6.34×10^{-4}

Table III: *E-shaped Object,* $\ell = 1.5\lambda$, $\tau = 0.05$ - Reconstruction errors: total (ξ_{tot}), internal (ξ_{int}) and external (ξ_{ext}) errors.

	$SNR = 50dB$			
	$S = 1$	$S = 2$	$S = 3$	$S = 4$
$L^{(S)}$	6.00	3.60	1.80	1.80
$N^{(S)}$	100	208	208	208
$Q^{(S)}$	100	144	36	36
	$SNR = 20dB$			
	$S = 1$	$S = 2$	$S = 3$	$S = 4$
$L^{(S)}$	6.00	3.60	2.10	1.80
$N^{(S)}$	100	208	208	208
$Q^{(S)}$	100	144	49	36
	$SNR = 10dB$			
	$S = 1$	$S = 2$	$S = 3$	$S = 4$
$L^{(S)}$	6.00	3.60	2.10	1.80
$N^{(S)}$	100	208	208	208
$Q^{(S)}$	100	144	49	36
	$SNR = 5dB$			
	$S = 1$	$S = 2$	$S = 3$	$S = 4$
$L^{(S)}$	6.00	3.60	2.10	1.80
$N^{(S)}$	100	208	208	208
$Q^{(S)}$	100	144	49	36

Table IV: *E-shaped Object,* $\ell = 1.5\lambda$, $\tau = 0.05$ - Investigation domain parameters: restricted investigation domain size $L^{(S)}$, total number of cells $N^{(S)}$ and number of cells within the restricted domain size $Q^{(S)}$.

ELEDIA Research Center

1.1.3 E-shaped Object, $\ell = 1.5\lambda$, $\tau = 0.15$ - IMSA-BCS reconstructed profiles

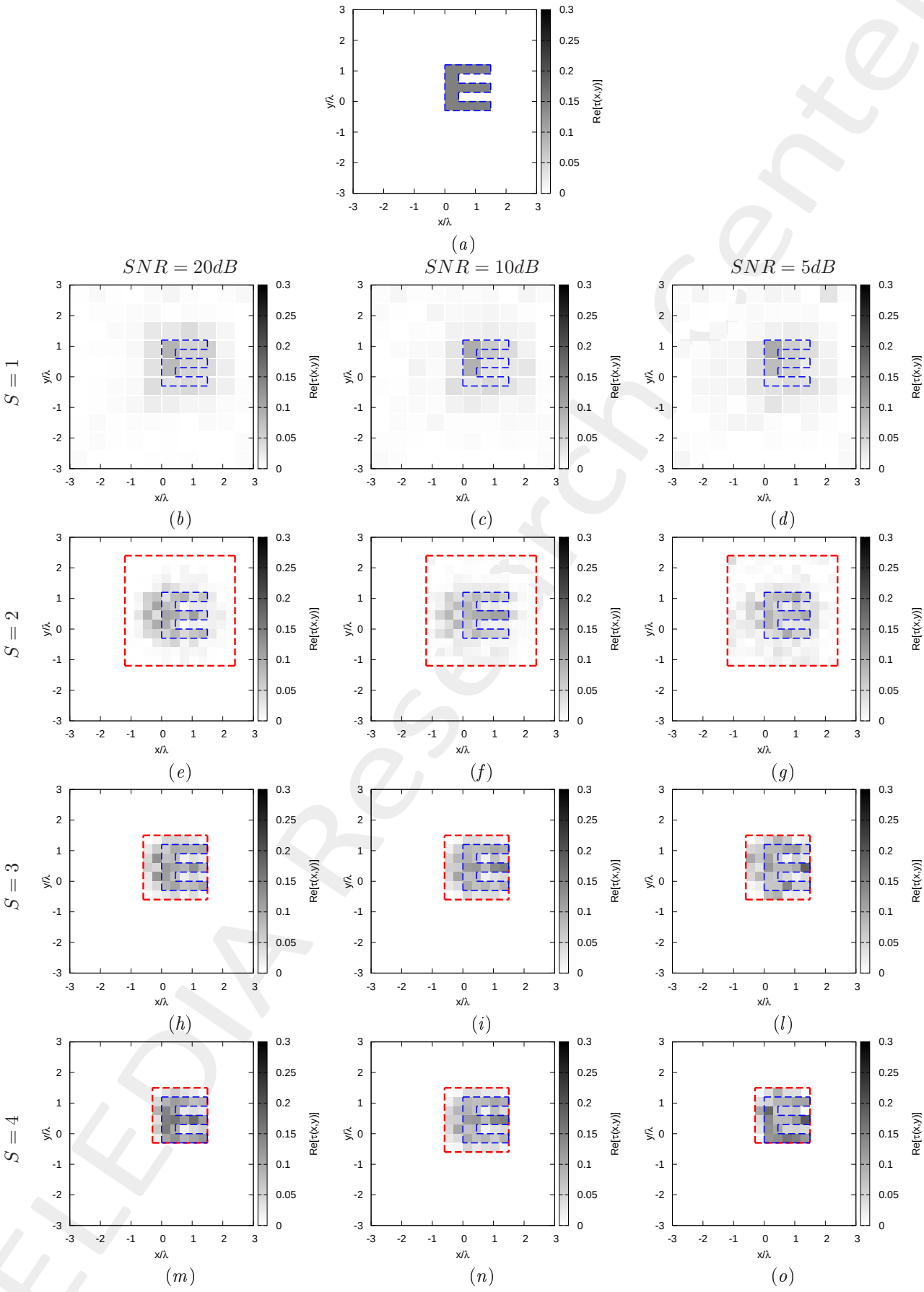

Figure 3: *E-shaped Object*, $\tau = 0.15$ - (a) Actual profile and (b)-(o) IMSA-BCS reconstructed profiles for $(b)(e)(h)(m)$ $SNR = 20$ [dB], $(c)(f)(i)(n)$ $SNR = 10$ [dB] and $(d)(g)(l)(o)$ $SNR = 5$ [dB] at the step (b)-(d) $S = 1$, (e)-(g) $S = 2$, (h)-(l) $S = 3$ and (m)-(o) $S = 4$.

ELEDIA Research Center

	$SNR = 50dB$			
	$S = 1$	$S = 2$	$S = 3$	$S = 4$
ξ_{tot}	1.21×10^{-2}	7.55×10^{-3}	5.64×10^{-3}	4.03×10^{-3}
ξ_{int}	7.71×10^{-2}	6.78×10^{-2}	4.98×10^{-2}	4.09×10^{-2}
ξ_{ext}	8.32×10^{-3}	4.16×10^{-3}	3.12×10^{-3}	1.78×10^{-3}
	$SNR = 20dB$			
	$S = 1$	$S = 2$	$S = 3$	$S = 4$
ξ_{tot}	1.23×10^{-2}	7.51×10^{-3}	5.59×10^{-3}	3.80×10^{-3}
ξ_{int}	7.75×10^{-2}	6.77×10^{-2}	4.97×10^{-2}	3.13×10^{-2}
ξ_{ext}	8.35×10^{-3}	4.16×10^{-3}	3.12×10^{-3}	1.89×10^{-3}
	$SNR = 10dB$			
	$S = 1$	$S = 2$	$S = 3$	$S = 4$
ξ_{tot}	1.28×10^{-2}	7.63×10^{-3}	5.61×10^{-3}	5.61×10^{-3}
ξ_{int}	7.67×10^{-2}	6.68×10^{-2}	4.88×10^{-2}	4.88×10^{-2}
ξ_{ext}	8.75×10^{-3}	4.27×10^{-3}	3.11×10^{-3}	3.11×10^{-3}
	$SNR = 5dB$			
	$S = 1$	$S = 2$	$S = 3$	$S = 4$
ξ_{tot}	1.50×10^{-2}	8.99×10^{-3}	6.64×10^{-3}	4.67×10^{-3}
ξ_{int}	7.74×10^{-2}	6.87×10^{-2}	5.41×10^{-2}	3.57×10^{-2}
ξ_{ext}	9.66×10^{-3}	5.06×10^{-3}	3.43×10^{-3}	2.18×10^{-3}

Table V: *E-shaped Object,* $\tau = 0.10$ - Reconstruction errors: total (ξ_{tot}), internal (ξ_{int}) and external (ξ_{ext}) errors.

	$SNR = 50dB$			
	$S = 1$	$S = 2$	$S = 3$	$S = 4$
$L^{(S)}$	6.00	3.60	2.10	1.80
$N^{(S)}$	100	208	208	208
$Q^{(S)}$	100	144	49	36
	$SNR = 20dB$			
	$S = 1$	$S = 2$	$S = 3$	$S = 4$
$L^{(S)}$	6.00	3.60	2.10	1.80
$N^{(S)}$	100	208	208	208
$Q^{(S)}$	100	144	49	36
	$SNR = 10dB$			
	$S = 1$	$S = 2$	$S = 3$	$S = 4$
$L^{(S)}$	6.00	3.60	2.10	2.10
$N^{(S)}$	100	208	208	208
$Q^{(S)}$	100	144	49	49
	$SNR = 5dB$			
	$S = 1$	$S = 2$	$S = 3$	$S = 4$
$L^{(S)}$	6.00	3.60	2.10	1.80
$N^{(S)}$	100	208	208	208
$Q^{(S)}$	100	144	49	36

Table VI: *E-shaped Object,* $\tau = 0.15$ - Investigation domain parameters: restricted investigation domain size $L^{(S)}$, total number of cells $N^{(S)}$ and number of cells within the restricted domain size $Q^{(S)}$.

ELEDIA Research Center

1.1.4 E-shaped Object, $\ell = 1.5\lambda$, $\tau = 0.20$ - IMSA-BCS reconstructed profiles

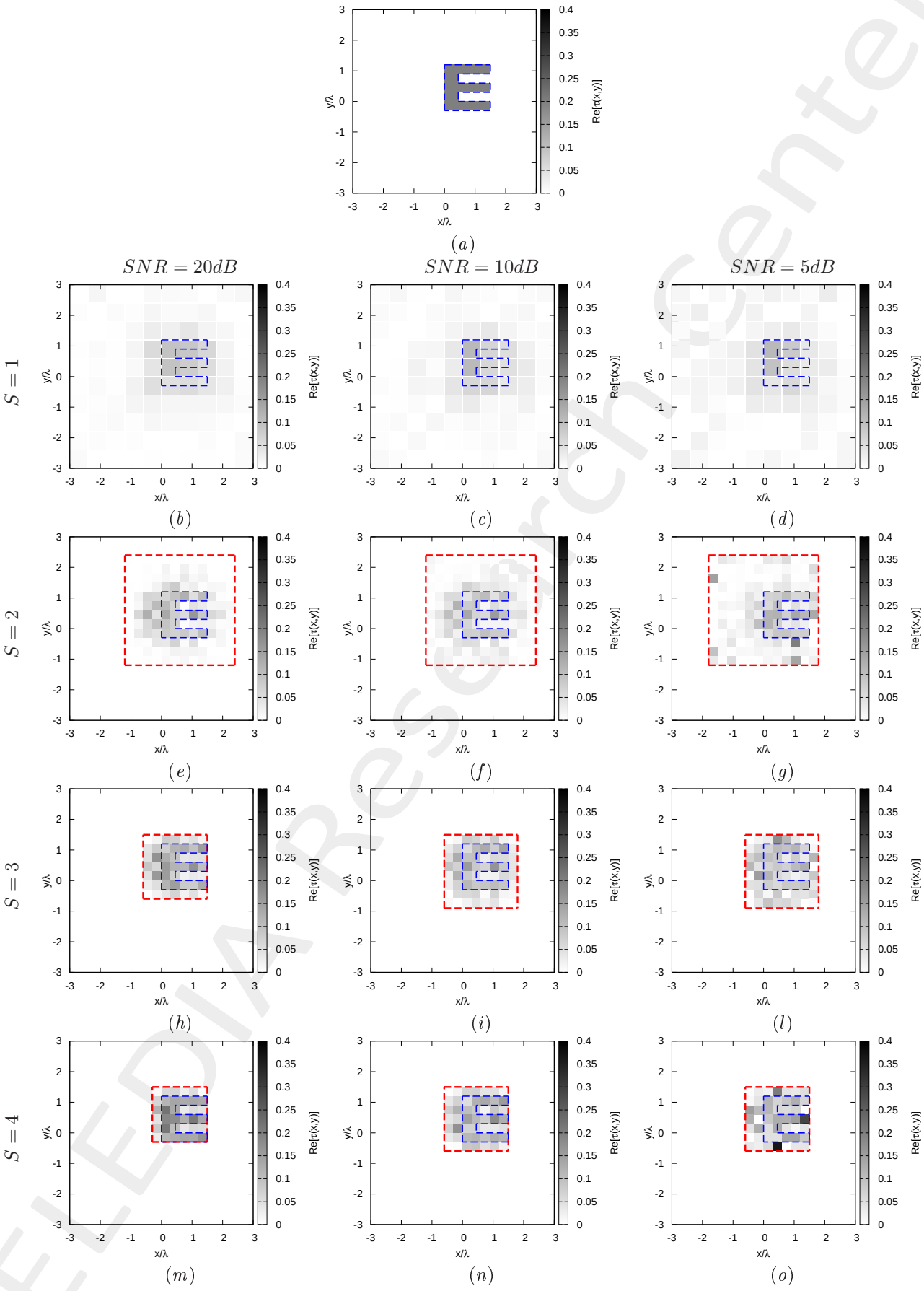

Figure 4: *E-shaped Object*, $\tau = 0.20$ - (a) Actual profile and (b)-(o) IMSA-BCS reconstructed profiles for $(b)(e)(h)(m)$ $SNR = 20$ [dB], $(c)(f)(i)(n)$ $SNR = 10$ [dB] and $(d)(g)(l)(o)$ $SNR = 5$ [dB] at the step (b)-(d) $S = 1$, (e)-(g) $S = 2$, (h)-(l) $S = 3$ and (m)-(o) $S = 4$.

ELEDIA Research Center

	$SNR = 50dB$			
	$S = 1$	$S = 2$	$S = 3$	$S = 4$
ξ_{tot}	1.65×10^{-2}	1.00×10^{-2}	7.38×10^{-3}	5.14×10^{-3}
ξ_{int}	1.03×10^{-1}	8.94×10^{-2}	6.43×10^{-2}	4.33×10^{-2}
ξ_{ext}	1.09×10^{-2}	5.41×10^{-3}	3.88×10^{-3}	2.23×10^{-3}
	$SNR = 20dB$			
	$S = 1$	$S = 2$	$S = 3$	$S = 4$
ξ_{tot}	1.67×10^{-2}	1.02×10^{-2}	7.64×10^{-3}	5.42×10^{-3}
ξ_{int}	1.04×10^{-1}	9.18×10^{-2}	6.70×10^{-2}	4.39×10^{-2}
ξ_{ext}	1.11×10^{-2}	5.53×10^{-3}	4.07×10^{-3}	2.52×10^{-3}
	$SNR = 10dB$			
	$S = 1$	$S = 2$	$S = 3$	$S = 4$
ξ_{tot}	1.75×10^{-2}	1.13×10^{-2}	9.45×10^{-3}	8.31×10^{-3}
ξ_{int}	1.01×10^{-1}	9.75×10^{-2}	8.30×10^{-2}	7.27×10^{-2}
ξ_{ext}	1.16×10^{-2}	6.19×10^{-3}	5.08×10^{-3}	4.44×10^{-3}
	$SNR = 5dB$			
	$S = 1$	$S = 2$	$S = 3$	$S = 4$
ξ_{tot}	2.32×10^{-2}	1.70×10^{-2}	1.20×10^{-2}	1.15×10^{-2}
ξ_{int}	1.06×10^{-1}	9.35×10^{-2}	9.31×10^{-2}	8.38×10^{-2}
ξ_{ext}	1.47×10^{-2}	8.66×10^{-3}	6.16×10^{-3}	5.40×10^{-3}

Table VII: *E-shaped Object,* $\tau = 0.20$ - Reconstruction errors: total (ξ_{tot}), internal (ξ_{int}) and external (ξ_{ext}) errors.

	$SNR = 50dB$			
	$S = 1$	$S = 2$	$S = 3$	$S = 4$
$L^{(S)}$	6.00	3.60	2.10	1.80
$N^{(S)}$	100	208	208	208
$Q^{(S)}$	100	144	49	36
	$SNR = 20dB$			
	$S = 1$	$S = 2$	$S = 3$	$S = 4$
$L^{(S)}$	6.00	3.60	2.10	1.80
$N^{(S)}$	100	208	208	208
$Q^{(S)}$	100	144	49	36
	$SNR = 10dB$			
	$S = 1$	$S = 2$	$S = 3$	$S = 4$
$L^{(S)}$	6.00	3.60	2.40	2.10
$N^{(S)}$	100	208	208	208
$Q^{(S)}$	100	144	64	49
	$SNR = 5dB$			
	$S = 1$	$S = 2$	$S = 3$	$S = 4$
$L^{(S)}$	6.00	3.60	2.39	2.10
$N^{(S)}$	100	208	208	208
$Q^{(S)}$	100	144	64	49

Table VIII: *E-shaped Object,* $\tau = 0.20$ - Investigation domain parameters: restricted investigation domain size $L^{(S)}$, total number of cells $N^{(S)}$ and number of cells within the restricted domain size $Q^{(S)}$.

ELEDIA Research Center

1.1.5 E-shaped Object, $\ell = 1.5\lambda$, $\tau = 0.20$ - IMSA-BCS multi-resolution grids

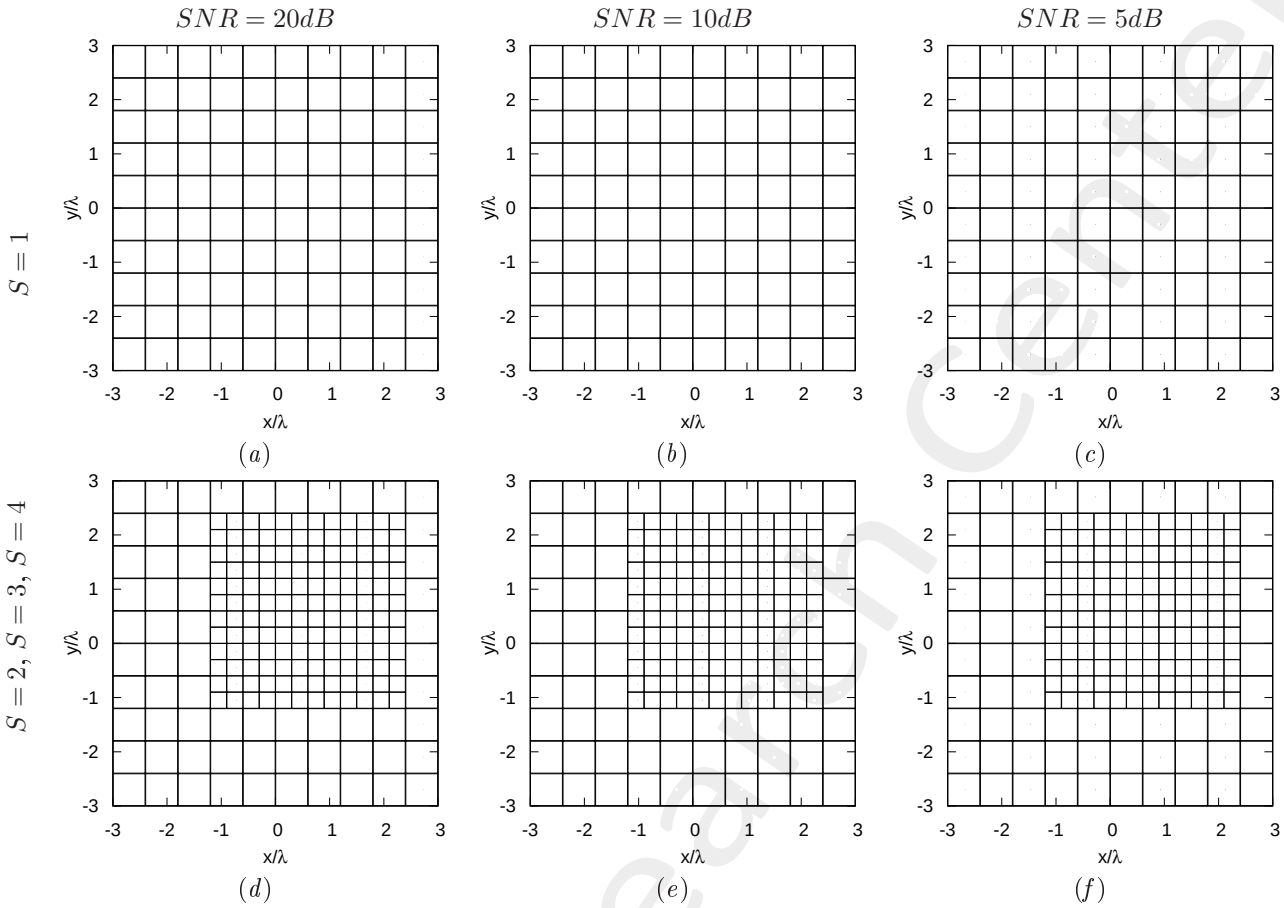

Figure 5: *E-shaped Object*, $\tau = 0.20$ - Example of (b)-(o) IMSA-BCS multi-resolution grids $(b)(e)(h)(m)$ $SNR = 20$ [dB], $(c)(f)(i)(n)$ $SNR = 10$ [dB] and $(d)(g)(l)(o)$ $SNR = 5$ [dB] at the step (b)-(d) $S = 1$, (e)-(g) $S = 2$, (h)-(l) $S = 3$ and (m)-(o) $S = 4$.

ELEDIA Research Center

1.2 Hollow Square, $\ell = 1.5\lambda$

Test Case Description

Direct solver:

- Side of the investigation domain: $L = 6.0\lambda$
- Cubic domain divided in $\sqrt{D} \times \sqrt{D}$ cells
- Number of cells for the direct solver: $D = 1600$ (discretization = $\lambda/10$)

Investigation domain:

- Cubic domain divided in $\sqrt{N} \times \sqrt{N}$ cells
- Number of cells for the inversion:
  - First Step IMSA: $N^{(1)} = 100$ (discretization = $\lambda/10$)
  - Following Steps IMSA: $N^{(i)}$ not fixed, defined according to the estimated RoI $\mathcal{D}^{(i)}$

Measurement domain:

- Total number of measurements: $M = 60$
- Measurement points placed on circles of radius $\rho = 4.5\lambda$

Sources:

- Plane waves
- Number of views: $V = 60$; $\theta_{inc}^{v} = 0^\circ + (v-1) \times (360/V)$
- Amplitude: $A = 1.0$
- Frequency: $F = 300$ MHz ($\lambda = 1$)

Background:

- $\varepsilon_r = 1.0$
- $\sigma = 0$ [S/m]

Scatterer

- Hollow square object, $\ell = 1.5\lambda$
- $\varepsilon_r \in \{1.01, 1.02, 1.04, 1.05, 1.06, 1.08, 1.10, 1.15, 1.20\}$
- $\sigma = 0$ [S/m]

ELEDIA Research Center

1.2.1 Hollow Square, $\ell = 1.5\lambda$, $\tau = 0.02$ - IMSA-BCS reconstructed profiles

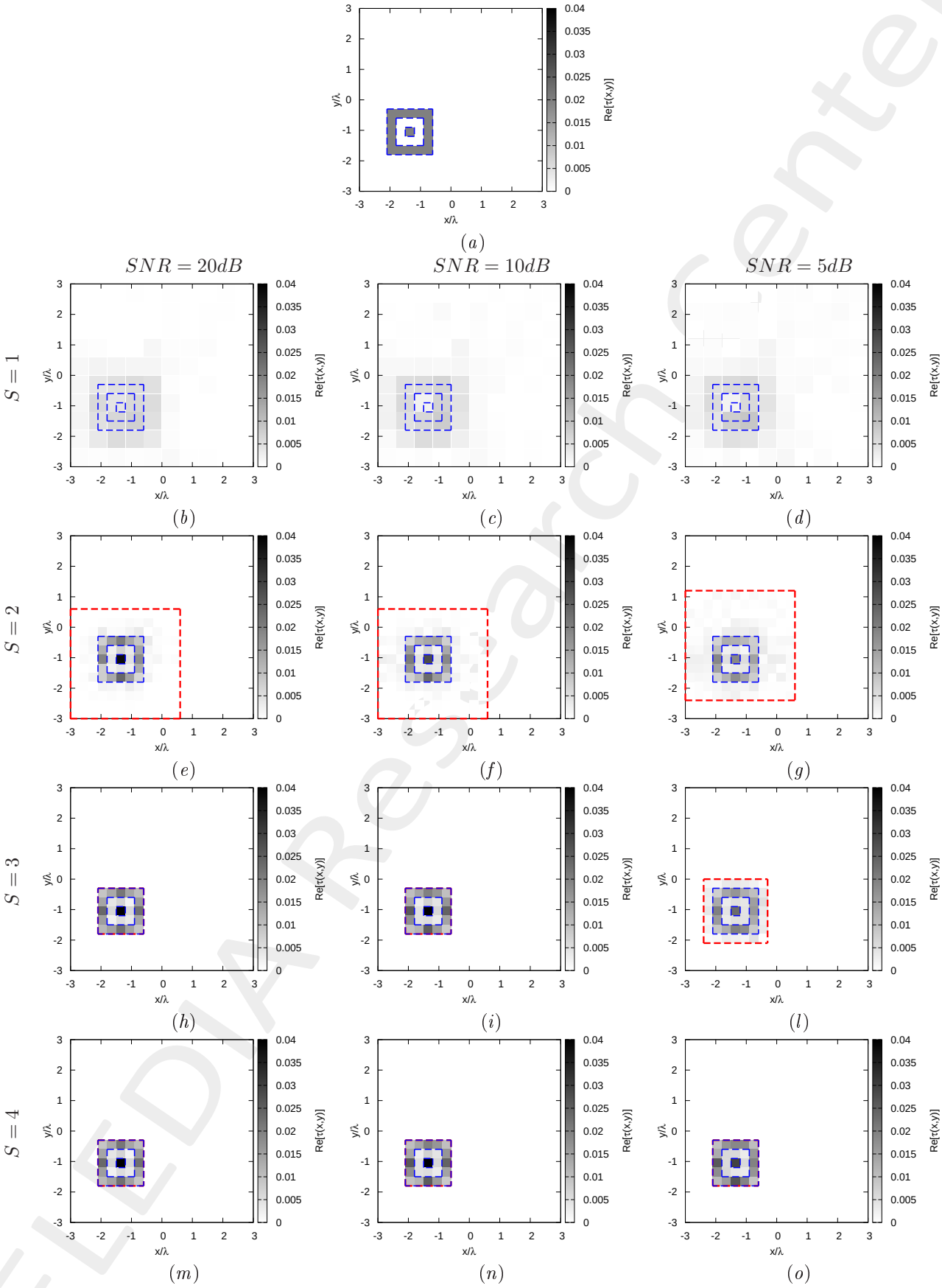

Figure 6: *Hollow Square*, $\ell = 1.5\lambda$, $\tau = 0.02$ - (a) Actual profile and (b)-(o) IMSA-BCS reconstructed profiles for $(b)(e)(h)(m)$ $SNR = 20$ [dB], $(c)(f)(i)(n)$ $SNR = 10$ [dB] and $(d)(g)(l)(o)$ $SNR = 5$ [dB] at the step (b)-(d) $S = 1$, (e)-(g) $S = 2$, (h)-(l) $S = 3$ and (m)-(o) $S = 4$.

FEDIA Research Center

	$SNR = 50dB$			
	$S = 1$	$S = 2$	$S = 3$	$S = 4$
ξ_{tot}	1.49×10^{-3}	4.97×10^{-4}	3.95×10^{-4}	3.95×10^{-4}
ξ_{int}	1.42×10^{-2}	7.65×10^{-3}	7.21×10^{-3}	7.21×10^{-3}
ξ_{ext}	9.12×10^{-4}	1.79×10^{-4}	9.24×10^{-5}	9.24×10^{-5}
	$SNR = 20dB$			
	$S = 1$	$S = 2$	$S = 3$	$S = 4$
ξ_{tot}	1.46×10^{-3}	5.06×10^{-4}	3.97×10^{-4}	3.97×10^{-4}
ξ_{int}	1.39×10^{-2}	7.49×10^{-3}	7.16×10^{-3}	7.16×10^{-3}
ξ_{ext}	8.87×10^{-4}	1.94×10^{-4}	9.69×10^{-5}	9.69×10^{-5}
	$SNR = 10dB$			
	$S = 1$	$S = 2$	$S = 3$	$S = 4$
ξ_{tot}	1.47×10^{-3}	5.05×10^{-4}	3.87×10^{-4}	3.87×10^{-4}
ξ_{int}	1.35×10^{-2}	6.77×10^{-3}	6.85×10^{-3}	6.85×10^{-3}
ξ_{ext}	9.05×10^{-4}	2.24×10^{-4}	1.00×10^{-4}	1.00×10^{-4}
	$SNR = 5dB$			
	$S = 1$	$S = 2$	$S = 3$	$S = 4$
ξ_{tot}	1.52×10^{-3}	6.77×10^{-4}	4.81×10^{-4}	3.23×10^{-4}
ξ_{int}	1.35×10^{-2}	7.82×10^{-3}	5.80×10^{-3}	5.21×10^{-3}
ξ_{ext}	9.54×10^{-4}	3.49×10^{-4}	2.42×10^{-4}	1.05×10^{-4}

Table IX: *Hollow Square*, $\ell = 1.5\lambda$, $\tau = 0.20$ - Reconstruction errors: total (ξ_{tot}), internal (ξ_{int}) and external (ξ_{ext}) errors.

	$SNR = 50dB$			
	$S = 1$	$S = 2$	$S = 3$	$S = 4$
$L^{(S)}$	6.00	1.50	1.50	1.50
$N^{(S)}$	100	208	208	208
$Q^{(S)}$	100	144	25	25
	$SNR = 20dB$			
	$S = 1$	$S = 2$	$S = 3$	$S = 4$
$L^{(S)}$	6.00	1.50	1.50	1.50
$N^{(S)}$	100	208	208	208
$Q^{(S)}$	100	144	25	25
	$SNR = 10dB$			
	$S = 1$	$S = 2$	$S = 3$	$S = 4$
$L^{(S)}$	6.00	1.50	1.50	1.50
$N^{(S)}$	100	208	208	208
$Q^{(S)}$	100	144	25	25
	$SNR = 5dB$			
	$S = 1$	$S = 2$	$S = 3$	$S = 4$
$L^{(S)}$	6.00	1.50	1.50	1.50
$N^{(S)}$	100	208	208	208
$Q^{(S)}$	100	144	49	25

Table X: *Hollow Square*, $\ell = 1.5\lambda$, $\tau = 0.02$ - Investigation domain parameters: restricted investigation domain size $L^{(S)}$, total number of cells $N^{(S)}$ and number of cells within the restricted domain size $Q^{(S)}$.

ELEDIA Research Center

References

[1] M. Salucci, G. Oliveri, and A. Massa, "GPR prospecting through an inverse scattering frequency-hopping multi-focusing approach," *IEEE Trans. Geosci. Remote Sens.*, vol. 53, no. 12, pp. 6573-6592, Dec. 2015.

[2] M. Salucci, L. Poli, N. Anselmi, and A. Massa, "Multifrequency Particle Swarm Optimization for enhanced multiresolution GPR microwave imaging," *IEEE Trans. Geosci. Remote Sens.*, vol. 55, no. 3, pp. 1305-1317, Mar. 2017.

[3] M. Salucci, L. Poli, and A. Massa, "Advanced multi-frequency GPR data processing for non-linear deterministic imaging," *Signal Processing* - Special Issue on 'Advanced Ground-Penetrating Radar Signal-Processing Techniques,' vol. 132, pp. 306-318, Mar. 2017.

[4] N. Anselmi, G. Oliveri, M. Salucci, and A. Massa, "Wavelet-based compressive imaging of sparse targets," *IEEE Trans. Antennas Propag.*, vol. 63, no. 11, pp. 4889-4900, Nov. 2015.

[5] G. Oliveri, M. Salucci, N. Anselmi, and A. Massa, "Compressive sensing as applied to inverse problems for imaging: theory, applications, current trends, and open challenges," *IEEE Antennas Propag. Mag.* - Special Issue on "Electromagnetic Inverse Problems for Sensing and Imaging," vol. 59, no. 5, pp. 34-46, Oct. 2017.

[6] A. Massa, P. Rocca, and G. Oliveri, "Compressive sensing in electromagnetics - A review," *IEEE Antennas Propag. Mag.*, pp. 224-238, vol. 57, no. 1, Feb. 2015.

[7] N. Anselmi, L. Poli, G. Oliveri, and A. Massa, "Iterative multi-resolution bayesian CS for microwave imaging," *IEEE Trans. Antennas Propag.*, vol. 66, no. 7, pp. 3665-3677, Jul. 2018.

[8] N. Anselmi, G. Oliveri, M. A. Hannan, M. Salucci, and A. Massa, "Color compressive sensing imaging of arbitrary-shaped scatterers," *IEEE Trans. Microw. Theory Techn.*, vol. 65, no. 6, pp. 1986-1999, Jun. 2017.

[9] G. Oliveri, N. Anselmi, and A. Massa, "Compressive sensing imaging of non-sparse 2D scatterers by a total-variation approach within the Born approximation," *IEEE Trans. Antennas Propag.*, vol. 62, no. 10, pp. 5157-5170, Oct. 2014.

[10] L. Poli, G. Oliveri, and A. Massa, "Imaging sparse metallic cylinders through a local shape function Bayesian compressive sensing approach," *Journal of Optical Society of America A*, vol. 30, no. 6, pp. 1261-1272, 2013.

[11] L. Poli, G. Oliveri, F. Viani, and A. Massa, "MT-BCS-based microwave imaging approach through minimum-norm current expansion," *IEEE Trans. Antennas Propag.*, vol. 61, no. 9, pp. 4722-4732, Sep. 2013.

ELEDIA Research Center

[12] F. Viani, L. Poli, G. Oliveri, F. Robol, and A. Massa, "Sparse scatterers imaging through approximated multitask compressive sensing strategies," *Microwave Opt. Technol. Lett.*, vol. 55, no. 7, pp. 1553-1558, Jul. 2013.

[13] L. Poli, G. Oliveri, P. Rocca, and A. Massa, "Bayesian compressive sensing approaches for the reconstruction of two-dimensional sparse scatterers under TE illumination," *IEEE Trans. Geosci. Remote Sens.*, vol. 51, no. 5, pp. 2920-2936, May 2013.

[14] L. Poli, G. Oliveri, and A. Massa, "Microwave imaging within the first-order Born approximation by means of the contrast-field Bayesian compressive sensing," *IEEE Trans. Antennas Propag.*, vol. 60, no. 6, pp. 2865-2879, Jun. 2012.

[15] G. Oliveri, L. Poli, P. Rocca, and A. Massa, "Bayesian compressive optical imaging within the Rytov approximation," *Optics Letters*, vol. 37, no. 10, pp. 1760-1762, 2012.

[16] G. Oliveri, P. Rocca, and A. Massa, "A Bayesian compressive sampling-based inversion for imaging sparse scatterers," *IEEE Trans. Geosci. Remote Sens.*, vol. 49, no. 10, pp. 3993-4006, Oct. 2011.

[17] G. Oliveri, M. Salucci, and N. Anselmi, "Tomographic imaging of sparse low-contrast targets in harsh environments through matrix completion," *IEEE Trans. Microw. Theory Tech.*, vol. 66, no. 6, pp. 2714-2730, Jun. 2018.

[18] M. Salucci, A. Gelmini, L. Poli, G. Oliveri, and A. Massa, "Progressive compressive sensing for exploiting frequency-diversity in GPR imaging," *Journal of Electromagnetic Waves and Applications*, vol. 32, no. 9, pp. 1164- 1193, 2018.

ELEDIA Research Center